Three-Dimensional Underwater Target Tracking With Acoustic Sensor Networks

Gokhan Isbitiren and Ozgur B. Akan, *Senior Member, IEEE*

***Abstract*—Using traditional sonar arrays may be difficult and impractical in some mission-critical scenarios, because they should be mounted on or towed by a ship or a submersible. Alternatively, underwater acoustic sensor networks (UW-ASNs) offer a promising solution approach. In this paper, a target-tracking algorithm for UW-ASNs, i.e., 3-D underwater target tracking (3DUT), is presented. The objective of 3DUT is to collaboratively accomplish accurate tracking of underwater targets with minimum energy expenditure. Based on the time of arrival of the echoes from the target after transmitting acoustic pulses from the sensors, the ranges of the nodes to the target are determined, and trilateration is used to obtain the location of the target. The location and the calculated velocity of the target are then exploited to achieve tracking. To realize energy-effective target tracking, 3DUT incorporates a new target-movement-based duty-cycle mechanism. To avoid rapid depletion of the energy resources of boundary nodes due to continuous surveillance, 3DUT employs an adaptive procedure to find, designate, and activate new boundary nodes. Performance evaluation shows that 3DUT is a promising alternative to the traditional sonar-based target-tracking approaches, particularly for on-demand surveillance applications.**

***Index Terms*—Distributed sonar sensor networks, target tracking, underwater acoustic sensor networks (UW-ASNs).**

I. Introduction

DETECTING, classifying, and tracking underwater targets are indispensable parts of modern underwater defense systems. So far, various types of sound navigation and ranging (sonar) arrays have been used for this purpose, such as surface ship-hull-mounted sonar, submarine-hull-mounted sonar, side-scan sonar, and towed arrays [1]–[6]. These sonar arrays are generally mounted on or towed by a ship or a submersible [2], [3] or deployed prior to the application [4], which makes them unsuitable for on-demand tracking missions. Moreover, the platform that tows the array or on which the array is mounted is a single point of failure for the entire system.

In terms of surveillance, reconnaissance, and targeting, sensor networks stand as a promising technology. A specific case of sensor networks, i.e., underwater sensor networks (UWSNs), are envisioned to enable applications for oceanographic data collection, offshore exploration, assisted navigation, and tactical surveillance applications [7]. There are some studies for underwater target detection and tracking with UWSNs [8]–[14]. However, time synchronization between the sensor nodes are assumed to be realized through the global positioning system (GPS) mechanism in [8]–[10], which is hard to achieve with distributed underwater sensors. Instead of proposing a complete tracking scheme, only location estimation is discussed in [11]. The energy expenditure, which is very important for UWSNs, is not taken into account in [12]. In [13], the wake-up/sleep mechanism is used to select several nodes, and the valid measurement selecting mechanism is used to reduce the number of awake sensor nodes. However, a high number of uniformly distributed static sensors are utilized, which requires prior deployment of the sensors. In addition, tracking is considered in two dimensions only, which is an important limitation for practical applications. In [14], a maximum-likelihood estimation algorithm is proposed for underwater target size detection, and a complete tracking mechanism is not provided.

To achieve underwater target detection and tracking, the challenges of underwater acoustic communications must be taken into account. For example, the propagation delay in underwater is five orders of magnitude higher than the delay in terrestrial radio-frequency channels. Furthermore, the delay is variable, which causes some of the communication mechanisms to fail.

To address the aforementioned issues, we present the *3-D underwater target tracking* (3DUT) algorithm. Because 3DUT does not depend on the number of nodes and the algorithm runs even if the number of the nodes changes, it is scalable. Furthermore, because it does not necessitate large sonar arrays and surface vessels to pull the nodes, it is cost effective. Tracking starts when the acoustic noise of a target is detected by the sensor nodes. The distances of the sensor nodes to the target are estimated by transmitting acoustic pulses (ping) and employing the time-of-arrival (ToA) of the pings and the echoes. The location of the target is then obtained by employing trilateration. To achieve tracking, the velocity and the projected location of the target are calculated. Based on these calculations, the nodes along the path of the target are activated to continuously collect information about the target. This process continues until there is no signal that is received from the target. We assume that 3DUT tracks one target at a time.

One of the most important features of 3DUT is the 3-D localization and tracking of the target. 3DUT utilizes a tracking-aware adaptive duty-cycle mechanism based on the 3-D movement pattern of the target for minimum energy expenditure.

Manuscript received January 7, 2011; revised May 12, 2011; accepted June 29, 2011. Date of publication August 4, 2011; date of current version October 20, 2011. This work was supported in part by the Turkish Scientific and Technical Research Council Career Award under Grant 104E043 and by the Turkish National Academy of Sciences Distinguished Young Scientist Award Program. The review of this paper was coordinated by Prof. A. Jamalipour.

The authors are with the Next-Generation and Wireless Communications Laboratory, Department of Electrical and Electronics Engineering, Koc University, Istanbul 34450, Turkey (e-mail: akan@ku.edu.tr).

Color versions of one or more of the figures in this paper are available online at http://ieeexplore.ieee.org.

Digital Object Identifier 10.1109/TVT.2011.2163538

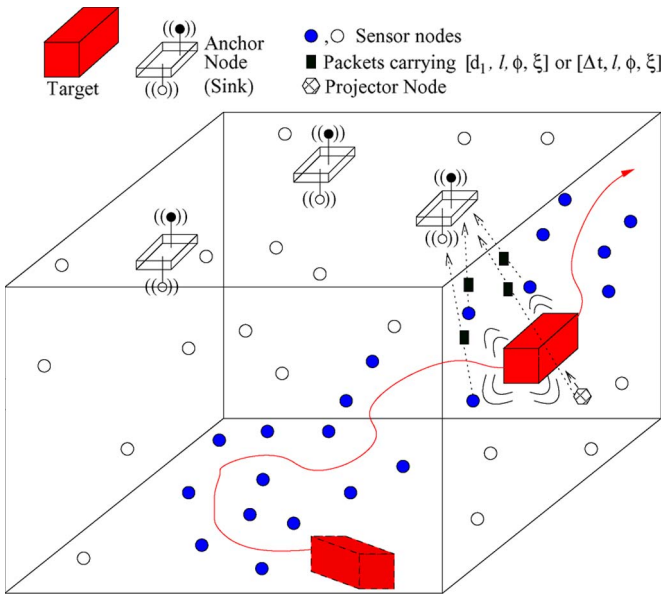

Fig. 1. Network model for a UW-ASN that implements 3DUT.

Moreover, 3DUT incorporates a new boundary node designation (BND) mechanism to minimize the time to detect the target when it enters into the sensing region by keeping it surrounded with higher duty-cycle nodes. Furthermore, time synchronization among the sensor nodes is not required for 3DUT operation.

The deployment of an underwater acoustic sensor network (UW-ASN) could be achieved by a helicopter or a surface platform. The sensor nodes are regarded as disposable and randomly distributed. Although there are tides and currents under the surface of the water, this assumption still holds through various mechanisms, i.e., attaching each underwater sensor node to a surface buoy [7] and using underwater vehicles [15] and underwater gliders [16] to hold the sensors at the expected underwater depths.

The remainder of this paper is organized as follows. In Section II, a 3DUT overview is given, and then, the steps of the algorithm are described. In Section III, first, possible reasons of errors are provided, and then, the simulation results of 3DUT are presented. Finally, this paper is concluded in Section IV.

II. Three-Dimensional Underwater Tracking Algorithm

The objective of the 3DUT algorithm is to detect, localize, and track submersibles such as submarines, torpedoes, and autonomous underwater vehicles in an accurate energy-efficient manner. One possible deployment of a 3-D UW-ASN is shown in Fig. 1. At least three anchor nodes float at the surface of the water to accomplish the localization of the underwater nodes [17]. One of these nodes is the sink, which collects the information from underwater sensor nodes and carries out the calculations. The nodes pointed out as dark circles are the nodes that collect and send information from the target to the sink. The hexagon-shaped node is the designated projector node, and it may change during the tracking process.

A. 3DUT Algorithm Overview

3DUT is a two-phase algorithm. During the first phase, *passive listening*, sensor nodes listen to the underwater environment for potential targets.

Once the noise that is radiated from a target has been detected, the second phase of the algorithm, *active ranging*, is initiated. To localize the target, 3DUT selects a projector node, which periodically sends pings, and the nodes use the ToA of the pings and their echoes to localize the target. By using the pings from the projector node, synchronization between the sensors is not necessary. The target is assumed to be a point target so that the echoes are isotropically radiated. During tracking, there is only one designated projector node, which can change with respect to the movement of the target. The ping contains a ping label l, which is used to identify the ping used in ranging calculations, as explained in Section II-C. Once the projector has received the echo, it calculates its distance to the target d_1. Then, it sends d_1, l, and its remaining energy (ξ) and coordinates (Φ) to the sink. All nodes have their location information through the localization algorithm, which periodically runs. There is no specific relation between 3DUT and the localization algorithm employed, i.e., one of the underwater localization algorithms in the literature [17], [18] can be used to achieve localization. Once the *hydrophone nodes* have received the echo, they calculate the time difference (Δt) between the arrival of the ping and the echo and send Δt, l, ξ, and Φ to the sink. The nodes that do not send but can receive the ping are called *hydrophone nodes*. Throughout the tracking, if the target gets out of the sensing region of the projector node, another projector is selected out of the hydrophone nodes.

The sink calculates the location, direction, and speed of the detected target (v), as explained in Sections II-C and D. Then, depending on the results of these calculations, it selects a new projector node and activates nodes that are located near the estimated trajectory of the target. Activating the nodes means sending an activation message, which includes a higher duty cycle δ and a new cycle period τ, which are determined based on the speed of the target, as explained in Section II-D.

To save energy, nodes that are not located at the network edge have low duty cycles. Nodes that are at the boundary of the sensing region have higher duty cycles to immediately detect the target that enters into the sensing region. Throughout the tracking process, the boundary nodes might become nonfunctional due to energy depletion; therefore, they send a message to the sink, notifying their status. The sink finds out the new boundary nodes, as explained in Section II-E, and sends a designation message to them. Hence, 3DUT achieves seamless surveillance of the sensor network zone.

B. Passive Listening

The sensor nodes check whether the intensity level (IL) that is caused by the received signal, which is radiated from an underwater target, is above a predefined detection threshold (DT) value. Let SL be the source level of the target, which is the radiated noise in the frequency band of interest, and PL be the underwater propagation loss of the acoustic signal. By

incorporating the basic sonar principles [1], the IL due to the target at the nodes is given by

$$IL = SL - PL. \tag{1}$$

The difference between the IL and the underwater noise (N) must be greater than DT to detect the target. To determine the PL, we consider the propagation loss of the sound under the surface of the water, which is given by

$$PL = 20 \log r + \alpha r \cdot 10^{-3} \tag{2}$$

where α is the attenuation coefficient (in decibels per kilometer), and r is the distance (in meters) [1]. To compare the difference between the IL caused by the target and the underwater noise with a predefined DT to understand whether there is a target, the noise component must be determined. Surface motion that is caused by the wind-driven waves is the major factor that contributes to the noise in the frequency region 100 Hz–100 kHz, which is the operating region used by the majority of acoustic systems [19]. Therefore, the noise parameter can be calculated as

$$10 \log N_\omega(f) = 50 + 7.5\omega^{1/2} + 20 \log f - 40 \log(f + 0.4) \tag{3}$$

where ω is the wind speed (in meters per second), and f is the frequency (in kilohertz) [19].

Initially, when the sensor nodes detect the target, they send a message to the sink node, indicating the detection of a target. The sink lists the nodes with respect to the time of reception of the detection message, i.e., target-to-node distance list. Then, the sink assigns the first node in the target-to-node distance list as the projector and broadcasts a message that indicates the new projector node. This way, the projector node is introduced to the sensors in the network. The sink node makes no calculations until it has received an acknowledgment (ACK) from the designated projector node. If the sink node does not receive an ACK, it waits for a timeout and again sends the designation message. The sink node repeats this process three times, and if it still does not receive an ACK, it designates the second node in the target-to-node distance list as the projector node and conducts the same procedure.

After the reception of a message from one of the boundary nodes, if the number of nodes that detect the target is less than 4, the sink sends direct activation messages to nodes that are close to the target. Note that the number of the active nodes, i.e., the nodes that collect information from the target, must be at least 4 to make the trilateration calculations in three dimensions. For this assumption to hold, at least one of the nodes must be on another plane than the other nodes. If the four nodes are on the same plane, the location of the target can be calculated at two different places. This approach is called flip ambiguity, which occurs for a graph in a d-D space when the positions of all neighbors of some vertex span a $(d-1)$-D space [20].

C. Active Ranging

During this phase, the projector node sends pings to the target, and the transmission rate of the ping is assumed to be $\gamma\ s^{-1}$, where s is given in seconds.

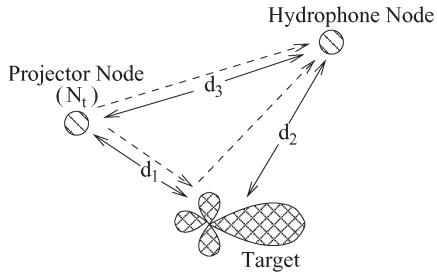

Fig. 2. Target-to-node distance calculation by utilizing a ping message.

In active sonar, the IL at the transmitter due to the target can be described as

$$IL = SL + TS - 2 \cdot PL \tag{4}$$

where SL is the source level, PL is the propagation loss, and TS is the target strength, which refers to the echo that is returned by an underwater target [1].

Nodes that receive the ping from the projector node and the echo from the target include the time difference of reception of the ping and the echo (Δt), whereas the projector node includes the distance between itself and the target (d_1) in the messages that they send to the sink. The messages also contain the locations of the nodes (Φ) for the sink to make target localization calculations, the ping label (l) for ping signal differentiation, and the remaining energies of the nodes (ξ) to let the sink node select the nodes to activate in the tracking process. The sink then calculates the location, direction, and speed of the target, as explained in this section and in Section II-D.

The target-to-node distances are calculated as in Fig. 2. Let N_t be the projector node and t_{Nt_1} and t'_{Nt_1} be the reception times of the echo from the target and the time of sending the ping, respectively. The distance between the target and N_t is calculated as

$$d_1 = C \cdot \left(t_{Nt_1} - t'_{Nt_1}\right)/2 \tag{5}$$

where C is the underwater speed of the sound. Each time a hydrophone node receives a ping with a label that is not previously received, it presets its timer. When the hydrophone node receives an echo with an already-received label, it timestamps the echo. Thus, the node obtains the difference of reception time (Δt) of the ping (t_P) and the echo t_T, which is given as

$$\Delta t = (d_1 + d_2)/C - d_3/C \tag{6}$$

where d_1, d_2, and d_3 are the distances between the projector node and the target, the hydrophone node and the target, and the projector node and the hydrophone node, respectively, as shown in Fig. 2. The distance between the hydrophone nodes and the target d_2 in (6) can be calculated as

$$d_2 = \Delta t \cdot C + d_3 - d_1. \tag{7}$$

N_t sends d_1, and the hydrophone nodes send Δt to the sink node, which has d_3 through localization, so that it calculates d_2.

After obtaining the distances between the nodes and the target, the sink node calculates the location of the target by using

the geometrical equation given by

$$(x_i - x_0)^2 + (y_i - y_0)^2 + (z_i - z_0)^2 = d_i^2 \quad (8)$$

where (x_i, y_i, z_i, d_i) are the coordinates of the node i and the distance between the node and the target, respectively, and (x_0, y_0, z_0) are the coordinates of the target. By exploiting four equations that are obtained by the information from four different sensor nodes, the location of the target is computed.

Note that the calculation of the location of the target must continuously be performed to achieve tracking.

D. Target-Tracking Mechanism

When the number of active nodes that provide information about the target to the sink node is at least 4, the location of the target is calculated by trilateration, as explained in Section II-C. After trilateration, the sink node calculates the velocity of the target by using its previous locations as

$$V_x = (x_2 - x_1)/(t_2 - t_1) \quad (9)$$

where V_x is the x-coordinate component of the velocity V_t of the target, (x_2, x_1) are the locations of the target at the x-coordinate at (t_2, t_1), and the y and z components are similarly calculated. If the target is about to leave the sensing region of at least one of the active nodes and the number of active nodes is not greater than 4, the sink node finds the total number of active nodes N_a whose sensing region the target is going to leave. Then, the sink calculates the path of the target by using its velocity and finds the nodes whose sensing regions intersect with the path of the target. The sink node sorts the nodes with respect to their distances to the target and selects the first N_a of the nodes for activation, which means increasing their duty cycles.

If the sink does not receive any message from the nodes that are expected to detect the target, it activates four new sensors that are the closest nodes to the target.

To obtain a new τ for a sensor node, the sink node calculates the time during which the target will be in the sensing region of that node, which is described as

$$t = \left(\left[(x_1 - x_0)^2 + (y_1 - y_0)^2 + (z_1 - z_0)^2 \right]^{1/2} \right) / V_t \quad (10)$$

where (x_0, y_0, z_0) and (x_1, y_1, z_1) are the coordinates from which the target enters into and exits from the sensing region of the sensor, respectively. τ is assumed to be the 1/4th the time that the target stays in the sensing region of the sensor node.

We use the sensing radius (SR) of the sensors to calculate the new δ, which can be given as

$$\delta = (0.67 \cdot 10^{-3} \cdot r)/\tau \quad (11)$$

where 0.67 is the propagation delay (in seconds per kilometer) [7], and r is the SR of the node (in meters). With this new duty-cycle value, the node is ensured to receive a signal during its active period from the target when the target is in the sensing region of the node.

The sink node selects another projector node when the target leaves the sensing region of the current projector node with the same mechanism described in Section II-B.

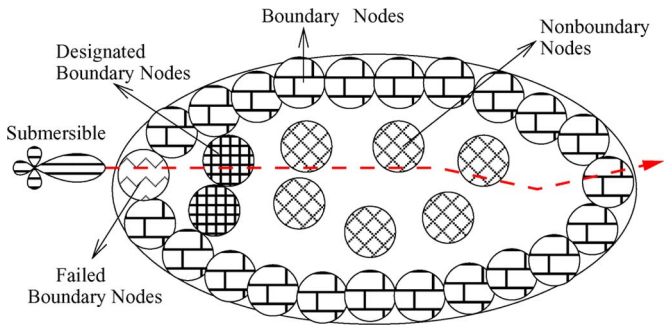

Fig. 3. When a boundary node fails, new boundary nodes are designated.

It is very important to detect the target as soon as it enters into the sensing region of the sensor network. To achieve this goal, the sensors at the boundary have higher duty cycles than the other sensors, as explained in the following discussion.

E. BND

The aim of BND is to keep the sensor network closed and bounded by the high-duty-cycle sensors. As shown in Fig. 3, if nodes are not designated and assigned as boundary nodes, the target may not be detected or tracked due to the low duty cycles of nonboundary nodes.

When a boundary node is about to run out of energy, it sends a failure alarm message to the sink node. After this message has been received or after the localization algorithm has been run, the sink node runs the BND algorithm to find the new boundary nodes.

In the first phase of the BND algorithm, 3DUT divides the sensing region into smaller cubes, which are called voxels. The dimensions of the voxels are selected with respect to the dimensions of the targets. The reason is that we assume that the sensing regions of two sensors intersect if the distance between the boundaries of their sensing regions is smaller than the minimum width of the target. We assume that the dimensions of the voxels are ν, which can be selected with respect to a practical value for the minimum width of a submarine [21].

The sink node first finds the coordinate limits of the region sensed by the nodes. As an example, the surfaces of the big cube in Fig. 4 are the limits of the region sensed by the nodes. Then, to check if a sensor, e.g., sensor 1 S_1, is at the boundary of the sensing region, the sink node finds the voxels that intersect with the sensors other than S_1 and marks them. Then, the sink finds the voxels that intersects with S_1. For S_1 to be at boundary of the sensing region, the voxels that intersect with S_1 must not be marked by other sensors, and they must not be enclosed by the voxels that are marked by other sensors. To check this condition, the sink starts from a voxel that intersects with only S_1. Then, the sink checks if it is possible to reach the nonmarked voxels at the boundary of the sensor network by iteratively selecting the nonmarked neighboring voxels. If it is possible, then S_1 is at the boundary, because it is not enclosed by the other sensors. This process is conducted for every sensor, and the boundary nodes are found. Because some of the nodes run out of energy, 3DUT keeps detecting and tracking the target with a sensor network whose sensing region becomes smaller.

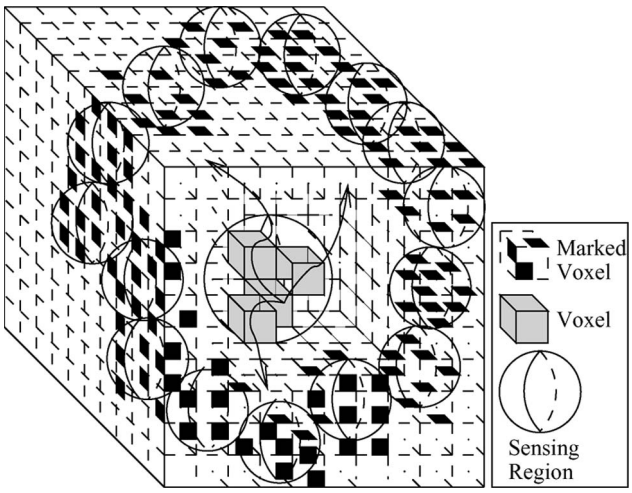

Fig. 4. BND algorithm.

The overall operations of the 3DUT algorithm are outlined in Algorithm 1.

Algorithm 1: Algorithm of the 3DUT protocol operation. $(x_{t_1}, y_{t_1}, z_{t_1})$ and $(x_{t_2}, y_{t_2}, z_{t_2})$ are the positions of the target at different times, $L_{1,2,3,4}$ are the locations of the sensor nodes, $d_{1,2,3,4}$ are the distances of the sensors to the target, and R is the SR of the nodes. d_s is the distance that the target will traverse in the sensing region of a new active sensor. N' are the nodes whose sensing regions overlap with the calculated path of the target. The activation message includes (δ, τ)

---

if $(SL - PL) - N \geq DT$ **then**
  projector selection
end if
if projector node **then**
  send ping periodically
  if Reception of an echo **then**
    calculate its distance to the target and send to the sink
  end if
end if
if hydrophone node **then**
  if Reception of a ping **then**
    preset timer
  end if
  if Reception of an echo **then**
    stop timer and send the Δt *to the sink*
  end if
end if
if Number of active nodes ≥ 4 **then**
  $Trilateration(d_1, d_2, d_3, d_4, L_1, L_2, L_3, L_4)$
  $Vx_t = (x_{t_2} - x_{t_1})/\Delta t,\ Vy_t = (y_{t_2} - y_{t_1})/\Delta t,\ Vz_t = (z_{t_2} - z_{t_1})/\Delta t$
else
  $\tau = d_s/4 \cdot V_t$
  $\delta = 0.67 \cdot 10^{-3} \cdot R/\tau$
  activate N'
end if
if the target exits from the sensing region of a projector node **then**
  select a projector node
end if
if Localization **then**
  $run\ BND$
end if
if Boundary nodes send a failure alarm message **then**
  $run\ BND$
end if

III. Performance Evaluation

We analyze the performance of the 3DUT algorithm with respect to the speed of sound, localization error, errors in distances between the nodes and the target, the number of nodes, and duty cycle. We deploy a simulation environment using ns-2 and distribute 50 sensors to an area of 600 m $\times$ 600 m $\times$ 600 m. We set the signal propagation speed to 1500 m/s. The attenuation of the underwater acoustic signal is adopted as explained in Section II-C.

A. Required Number of Nodes for Accurate Tracking

To track a target in the sensing region of sensors, all the subregions that form the whole sensing region must be covered by at least four sensors, i.e., it must be 4-covered. Before tracking, the sensors are randomly distributed as a result of a Poisson process [22]. Reformulating the results in [22] for 3-D space, the probability of full coverage in a 3-D arbitrary volume $(V_{\text{arbitrary}})$ becomes

$$P_{cov}^{3D} = 1 - e^{\frac{-8r^3\lambda}{V_{\text{arbitrary}}}} \tag{12}$$

where λ is the number of nodes. To ensure 1-coverage, the distance between two neighboring sensors should be less than $2r$ on the x-, y-, and z-axes, where r is the SR of the nodes. Hence, the total volume between two neighboring sensors should be less than $8r^3$.

The probability that k sensors will be present in the sensing region of a sensor is given by [22]

$$Pr_k = \frac{\left(\rho\frac{4}{3}\pi r^3\right)^k e^{-\rho\frac{4}{3}\pi r^3}}{k!} \tag{13}$$

where ρ is the node density. Combining (12) and (13), the probability that the specified arbitrary volume is covered by k or more sensor nodes is given by

$$\Pr = \left[1 - \sum_{k=0}^{k-1} \frac{\left(\rho\frac{4}{3}\pi r^3\right)^k e^{-\rho\frac{4}{3}\pi r^3}}{k!}\right]\left[1 - e^{\frac{-8r^3\lambda}{V_{\text{arbitrary}}}}\right]. \tag{14}$$

In Fig. 5, the probabilities of 4-coverage for different sensor numbers, SRs, and volumes are shown.

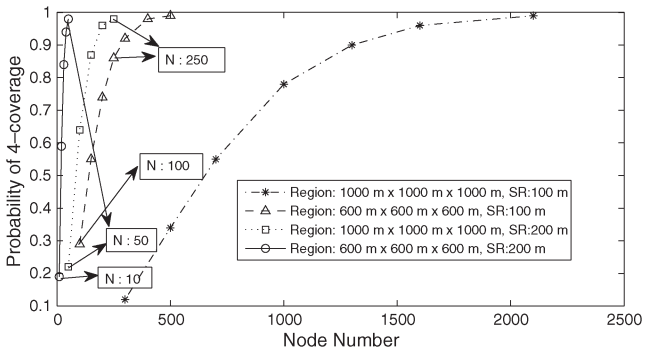

Fig. 5. Probability that any point in the region is covered by at least four sensors versus the number of nodes for different SRs.

B. Preliminary Error Analysis

In this section, we analyze the sources of errors in tracking and find out error bounds for the components of the sources of errors to obtain an overall error bound for 3DUT.

1) Sound Speed Error: C varies with respect to the temperature, pressure (depth), and salinity. C is computed by exploiting the empirical formula [1]

$$\begin{aligned} C(T,h,s) = {} & 1492.9 + 3(T-10) - 6\cdot 10^{-3}(T-10)^2 \\ & - 4\cdot 10^{-2}\cdot (T-18)^2 + 1.2(s-35) \\ & - 10^{-2}(T-18)(s-35) + \frac{h}{61} \end{aligned} \tag{15}$$

where T is the temperature (in Celsius), h is the depth (in meters), and s is the salinity (in parts per thousand). Hence, the error in C can be given as

$$\begin{aligned} \Delta C \leq {} & \frac{\partial C}{\partial T}\Delta T + \frac{\partial C}{\partial h}\Delta h + \frac{\partial C}{\partial s}\Delta s \\ = {} & \left[3 + 6\cdot 10^{-3}(2T-20) - (4\cdot 10^{-2})(2T-36)\right]\Delta T \\ & - 10^{-2}(s-35)\Delta T + \left[1.2 - 10^{-2}(T-18)\right]\Delta s + \frac{\Delta h}{61}. \end{aligned}$$

In [23], it is stated that Δs and ΔT can be assumed to be 0.75 ppt and 0.1 °C, respectively. The temperature and the depth can be obtained by the conductivity, temperature and depth sensors [24]. For $\Delta h = 2$ m, we obtain the upper bound for ΔC as 1.35 m/s at 10 °C and for a salinity of 35 ppt.

2) Target-to-Node Distance Accuracy: 3DUT calculates d_1 and d_2 by employing (5) and (7). The error bound in distance between the projector node and the target can be computed by

$$\begin{aligned} \Delta d_1 \leq {} & \frac{\partial d_1}{\partial C}\Delta C + \frac{\partial d_1}{\partial\left(t_{Nt_1} - t'_{Nt_1}\right)}\Delta\left(t_{Nt_1} - t'_{Nt_1}\right) \\ = {} & \left(t_{Nt_1} - t'_{Nt_1}\right)\frac{\Delta C}{2} + \frac{C}{2}\cdot\Delta\left(t_{Nt_1} - t'_{Nt_1}\right) \end{aligned} \tag{16}$$

where C is the underwater sound speed, and $(t_{Nt_1} - t_{Nt_1})'$ is the time difference between the reception of the echo and the transmission of the ping. The contribution of $\Delta(t_{Nt_1} - t_{Nt_1})'$, which is the error in the timer of the sensor, is neglected; hence, Δd_1 is due to ΔC, i.e., it changes with respect to the distance between the projector node and the target. The dependency of Δd_1 to d_1 at different ΔCs is given in Fig. 6. As shown in Fig. 6, Δd_1 increases as the distance between the projector and the target increases, because in this case, the propagation time of the signal to travel between the projector and the target increases, which amplifies the effect of ΔC.

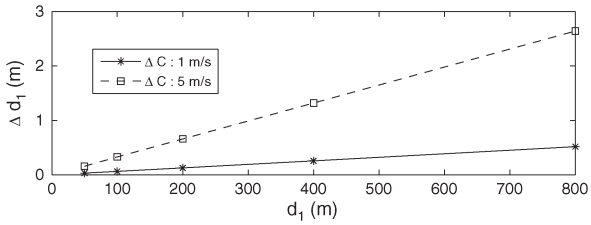

Fig. 6. Δd_1 versus d_1 for different ΔCs.

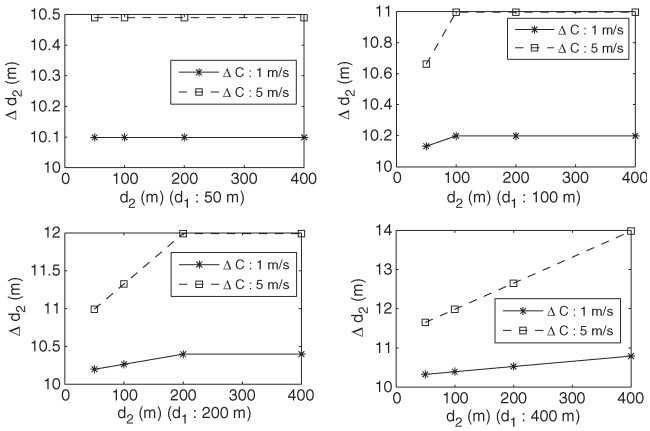

Fig. 7. Δd_2 versus d_2 for different d_1s and ΔCs.

The error bound in distance between the hydrophone nodes and the target can be computed by

$$\begin{aligned} \Delta d_2 \leq {} & \frac{\partial d_2}{\partial c}\Delta C + \frac{\partial d_2}{\partial(t_T - t_P)}\Delta(t_T - t_P) + \Delta d_3 + \Delta d_1 \\ = {} & (t_T - t_P)\cdot\Delta C + C\cdot\Delta(t_T - t_P) + \Delta d_3 + \Delta d_1 \end{aligned}$$

where t_T is the time of reception of the echo from the target, and t_P is the time of reception of the ping from the projector node by the hydrophone nodes. The contribution of $\Delta(t_T - t_P)$ can be neglected. The error in d_2 is composed of the error in the underwater sound speed, Δd_1, and Δd_3, which is the error incurred by the localization algorithm employed. The average error in the localization algorithm is assumed to be 5 m [17]. Because d_3 is the distance between two nodes, we assume that the maximum Δd_3 is 10 m. In Fig. 7, the change of Δd_2 with respect to d_2 at different ΔCs and d_1s is shown.

C. Detection Performance

We analyze the detection distances with respect to frequency and wind speed for different possible targets.

1) Passive Detection Performance: The behavior of the detection distances of the sensors, which can be calculated by (1)–(3) with respect to underwater noise and frequency, is shown in Fig. 8. The radiated noise values of the vessels in Fig. 8 with respect to frequency can be found in Table I [1].

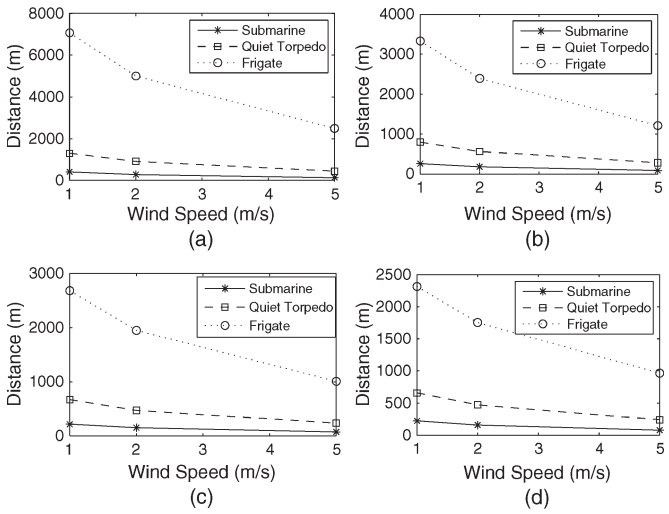

Fig. 8. Passive detection distance versus wind speed at frequencies (a) $f = 1$ kHz, (b) $f = 3$ kHz, (c) $f = 5$ kHz, and (d) $f = 10$ kHz.

TABLE I
RADIATED NOISE OF THE VESSELS AT DIFFERENT FREQUENCIES

Frequency (kHz)	*Submarine (dB)*	*Quiet torpedo (dB)*	*Frigate (dB)*
f = 1	110	120	135
f = 3	100	110	123
f = 5	95	105	118
f = 10	90	100	113

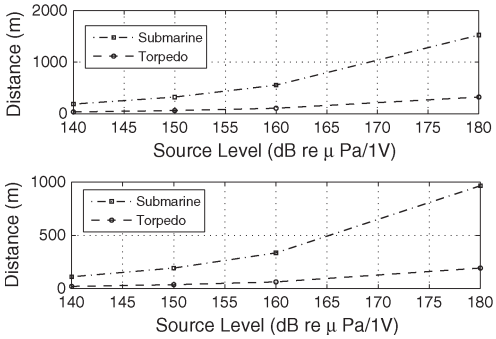

Fig. 9. Active detection distance versus source level at 10 kHz.

As observed in Fig. 8, the detection distance decreases as the wind speed increases, because the underwater ambient noise increases with the wind speed, as described in (3). As frequency increases, the noises of the devices decrease [1], and the propagation loss increases, which reduces the detection distance. However, as the frequency increases, the underwater ambient noise also decreases, which causes the detection distance to increase.

2) Active Detection Performance: As shown in Fig. 9, the detection distance increases as the source level increases. The detection distance of a submarine is higher than the torpedoes, because the target strength of a submarine is greater than the target strength of torpedoes.

D. Tracking Accuracy

We present the accuracy performance as the tracking error with respect to different metrics such as the number of nodes,

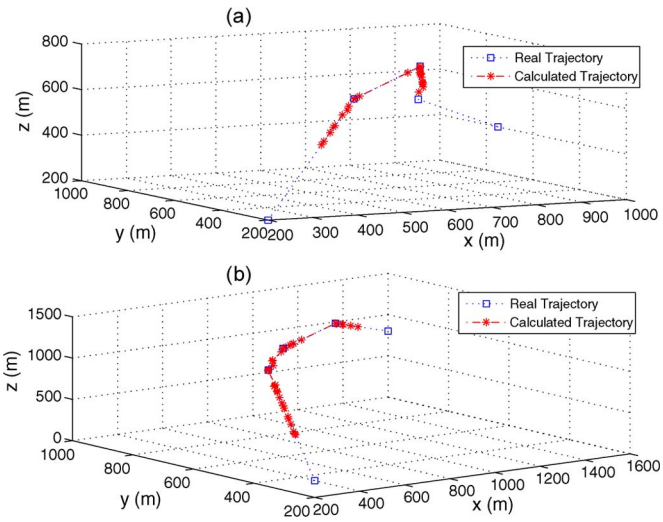

Fig. 10. Calculated target trajectories for different mobilities of the target.

underwater speed of sound, channel error rate, delay variance, localization error, and errors in distances between the nodes and the target. The tracking error is given as

$$E_{Avg} = \frac{1}{N}\sum_{i=1}^{N}\left[(x_i' - x_i)^2 + (y_i' - y_i)^2 + (z_i' - z_i)^2\right]^{1/2}$$

where E_{Avg} is the average error, N is the number of collected target location data, (x_i, y_i, z_i) is the real location of the target, and (x_i', y_i', z_i') is the calculated location of the target.

1) Accuracy versus the Number of Nodes: Because the information from the nodes is used to calculate the location of the target, intuitively, the accuracy of tracking improves as the number of nodes increases. However, this is not always the case, because 3DUT calculates the location of the target using the information from four different nodes. During tracking, although the target is in the sensing region of more than four nodes, the information from some of the nodes is not used. The average tracking error is simulated to be 4.53 m when there are 50 nodes and 9.61 m when there are 20 nodes.

2) Accuracy versus the Underwater Speed of Sound: As explained in Section III-B1, the speed of the sound may vary with respect to temperature, depth, and salinity. The average tracking error is found to be 7.94 m when there is a 5-m/s error in the underwater speed.

3) Effect of the Mobility of the Target and the Size of the Network: The mobility of the target affects the tracking error, because it determines the number of nodes involved in the tracking. As shown in Fig. 10, the target is not always tracked, because sometimes during tracking, it is not detected by at least four sensors, and the location of the target cannot be obtained.

In Fig. 10(a), the network area is 1000 m $\times$ 1000 m $\times$ 1000 m, and in Fig. 10(b), the network area is 2000 m $\times$ 2000 m $\times$ 2000 m. The average errors observed in these two settings are 10.2 and 10.5 m, respectively. Clearly, the simulation area does not directly affect the tracking error.

4) Effect of the Velocity of the Target: As the velocity of the target increases, the target stays less time in the sensing regions of the nodes; therefore, the active and projector nodes rapidly

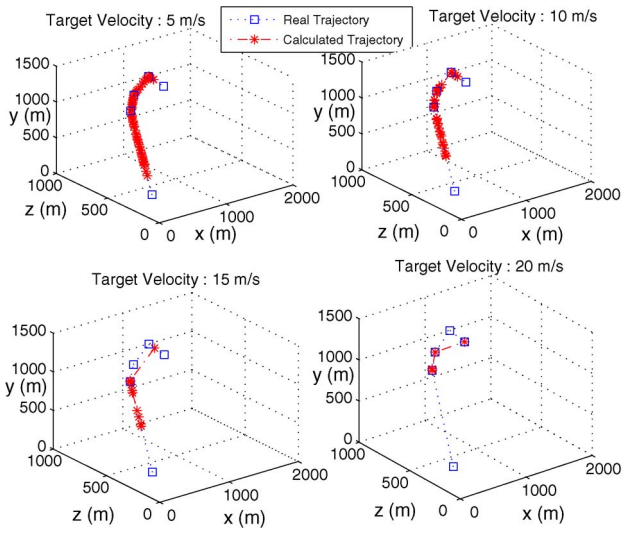

Fig. 11. Calculated target trajectories for different target speeds.

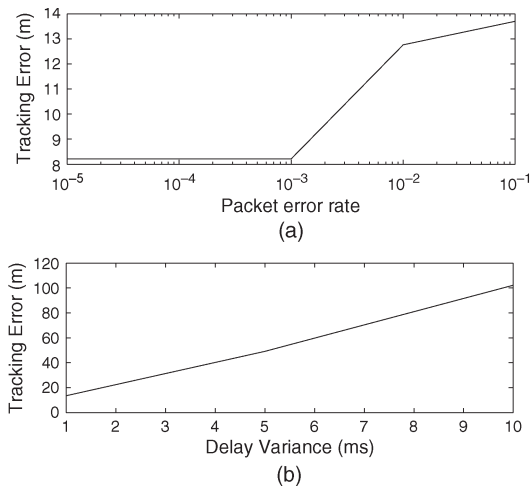

Fig. 12. Tracking error versus (a) packet error rate and (b) delay variance.

change. As a result, as the velocity increases, the number of calculations of the location of the target, i.e., the resolution of the tracking, decreases. The results shown in Fig. 11 are consistent with the intuition, and clearly, the resolution of tracking decreases as the speed of the target increases.

5) Accuracy versus Channel Error Rate and Delay Variance: As shown in Fig. 12(a), the accuracy decreases as the channel error rate increases. In addition, the underwater acoustic communication channel has highly varying delay, which incurs a high target localization error. As shown in Fig. 12(b), the tracking error increases when the delay variance increases.

6) Accuracy versus Error in the Localization of the Nodes: As shown in Fig. 13, when there is an average localization error (E_L) of 5 m, the tracking accuracy is seriously affected, and the sensor network missed a part of the path of the target. The average tracking error is computed to be 12.8 m.

7) Accuracy versus Δd_1*:* In the 3DUT algorithm, the location of the target and d_2 are a function of d_1. The average tracking error with respect to Δd_1 is shown in Table II. To reduce Δd_1, the error in the underwater sound speed must be minimized.

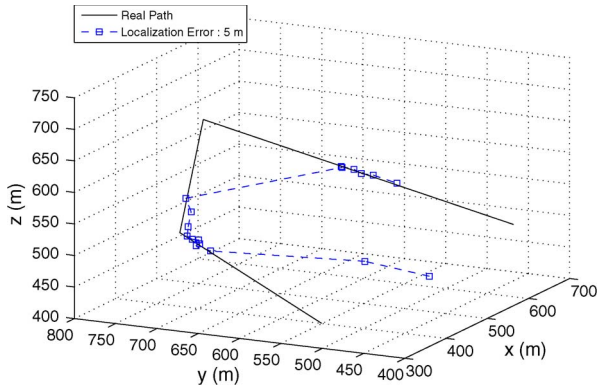

Fig. 13. Calculated target trajectory in case of localization errors.

TABLE II
ACCURACY (AVERAGE TRACKING ERROR) VERSUS E_L, Δd_1, Δd_2, AND v

Accuracy vs E_L	
	Average Tracking Error
E_L : 5 m	12.87 m
Accuracy vs Δd_1	
	Average Tracking Error
Δd_1 : 1 m	8.54 m
Δd_1 : 3 m	17.09 m
Accuracy vs Δd_2	
	Average Tracking Error
Δd_2 : 2 m, E_L : 5 m	12.89 m
Accuracy vs Target Speed(v)	
	Average Tracking Error
v : 5 m/s	7.74 m
v : 10 m/s	10.2 m
v : 15 m/s	14.78 m
v : 20 m/s	21.05 m

8) Accuracy versus Δd_2*:* In the 3DUT algorithm, the location of the target is a function of d_2. The average tracking error with respect to Δd_2 is shown in Table II. Running the simulations with different random error patterns, we obtain an average error of 12.89 m for Δd_2.

When we apply the maximum errors for the components such as Δd_1, Δd_2, ΔL, and packet loss probability and run the simulation, we obtain a maximum average error of 29.96 m. Compared with large submarine sizes such as 175 m [25], this error is acceptable for the localization of the target.

E. Energy Consumption

1) Effect of the BND Algorithm: We analyze the performance of BND by considering the cases with and without BND. In the first case, we use the BND algorithm, and we assign 50% and 25% duty cycles to the boundary nodes and nonboundary nodes, respectively. In the second case, we do not use the BND algorithm and assign 50% duty cycles to all the nodes. As shown in Fig. 14, for varying durations, using BND results in less energy consumption. The energy consumption decreases by an average value of 6%. Therefore, we conclude that BND is a promising approach for reducing energy consumption in target tracking with UWSNs.

2) Energy Consumption versus Duty Cycles: Based on the results in Fig. 15, the energy consumption decreases when lower duty cycles are used.

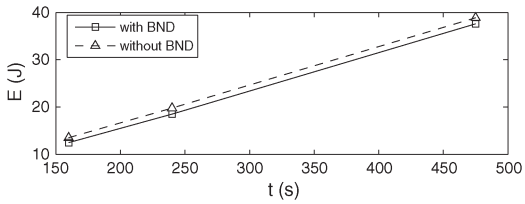

Fig. 14. BND energy consumption performance.

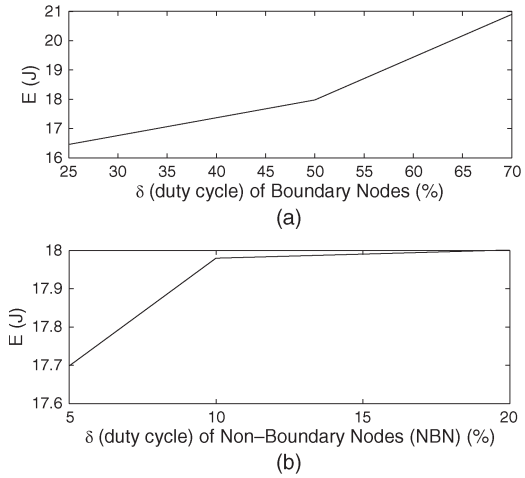

Fig. 15. Average energy consumption versus duty cycles. BN: Boundary node. NBN: Nonboundary node. (a) δ_{NBN}: 10%. (b) δ_{BN}: 50%.

IV. Conclusion

In this paper, 3DUT, which is a distributed energy-aware solution for the target-tracking problem for underwater domain, has been presented. Through analysis and simulations, we have presented that 3DUT can track the targets in an accurate energy-efficient manner. As the delay variance increases, the tracking error increases. Due to the channel error rate, some of the packets can be lost, which results in tracking errors. It is concluded that the tracking capability is related to the target's mobility pattern, because it affects the number of sensors employed in the tracking process. The target localization calculations are based on the locations of the sensors; therefore, the accuracy of the localization algorithm employed is very important. We compare the cases with and without BND and conclude that, by using BND, the average energy consumption decreases by 6%. The simulation results show that the average track error is around 7 m and that the maximum track error is less than 30 m, which is acceptable.

References

[1] A. D. Waite, *SONAR for Practicing Engineers*, 3rd ed. Hoboken, NJ: Wiley, 2001.
[2] D. Eickstedt, M. Benjamin, H. Schmidt, and J. Leonard, "Adaptive tracking of underwater targets with autonomous sensor networks," *J. Underwater Acoust.*, vol. 56, pp. 465–495, 2006, unclassified.
[3] M. I. Pettersson, V. Zetterberg, and I. Claesson, "Detection and imaging of moving targets in wideband SAS using fast time backprojection combined with space–time processing," in *Proc. MTS/IEEE Oceans*, 2005, vol. 3, pp. 2388–2393.
[4] E. Dalberg, A. Lauberts, R. K. Lennartsson, M. J. Levonen, and L. Persson, "Underwater target tracking by means of acoustic and electromagnetic data fusion," in *Proc. 9th Int. Conf. Inf. Fusion*, Florence, Italy, Jul. 2006, pp. 1–7.
[5] M. Asif, M. Rizal Arshad, and A. Yahya, "An active contour for underwater target tracking and navigation," in *Proc. Int. Conf. Man-Mach. Syst.*, Langkawi Islands, Malaysia, Sep. 2006, pp. 1–6.
[6] S. K. Rao, "Application of statistical estimators for underwater target tracking," in *Proc. IEEE/ION Position, Location, Navig. Symp.*, Apr. 2006, pp. 1040–1044.
[7] I. F. Akyildiz, D. Pompili, and T. Melodia, "Underwater acoustic sensor networks: Research challenges," *Ad Hoc Netw. (Elsevier)*, vol. 3, no. 3, pp. 257–279, May 2005.
[8] V. Zetterberg, M. I. Pettersson, and I. Claesson, "Comparison between whitened generalized cross correlation and adaptive filter for time delay estimation with scattered arrays for passive positioning of moving targets in Baltic Sea shallow waters," in *Proc. Oceans MTS/IEEE*, Washington, DC, Sep. 2005, pp. 2356–2361.
[9] V. Zetterberg, M. I. Pettersson, L. Tegborg, and I. Claesson, "Passive scattered array positioning method for underwater acoustic source," in *Proc. Oceans MTS/IEEE*, Sep. 2005, pp. 1–6.
[10] V. Zetterberg, M. I. Pettersson, L. Tegborg, and I. Claesson, "Acoustic passive 3-D imaging method for scattered arrays," in *Proc. UDT Pacific, Undersea Defence Technol. Conf.*, San Diego, CA, Dec. 2006.
[11] S. Zhou and P. Willett, "Submarine location estimation via a network of detection-only sensors," *IEEE Trans. Signal Process.*, vol. 55, no. 6, pp. 3104–3115, Jun. 2007.
[12] M. Hahn and J. Rice, "Undersea navigation via a distributed acoustic communication network," in *Proc. Turkish Int. Conf. Acoust.*, Istanbul, Turkey, Jul. 2005.
[13] C. Yu, K. Lee, J. Choi, and Y. Seo, "Distributed single target tracking in underwater wireless sensor networks," in *Proc. SICE Annu. Conf.*, Tokyo, Japan, Aug. 2008, pp. 1351–1356.
[14] Q. Liang and X. Cheng, "Underwater acoustic sensor networks: Target size detection and performance analysis," *Ad Hoc Netw. (Elsevier)*, vol. 7, no. 4, pp. 803–808, Jun. 2009.
[15] *AUV Laboratory at MIT Sea Grant*. [Online]. Available: http://auvlab.mit.edu/
[16] R. Davis, C. Eriksen, and C. Jones, "Autonomous buoyancy driven underwater gliders," in *The Technology and Applications of Autonomous Underwater Vehicles*, G. Griffiths, Ed. London, U.K.: Taylor & Francis, 2002.
[17] M. T. Isik and O. B. Akan, "A three-dimensional localization algorithm for underwater acoustic sensor networks," *IEEE Trans. Wireless Commun.*, vol. 8, no. 9, pp. 4457–4463, Sep. 2009.
[18] Z. Zhou, J. H. Cui, and S. Zhou, "Localization for large-scale underwater sensor networks," in *Proc. IFIP Netw.*, May 2007, pp. 108–119.
[19] M. Stojanovic, "On the relationship between capacity and distance in an underwater acoustic communication channel," in *Proc. ACM WUWNet*, Los Angeles, CA, Sep. 2006, pp. 41–47.
[20] D. Moore, J. Leonard, D. Rus, and S. Teller, "Robust distributed network localization with noisy range measurements," in *Proc. ACM SenSys*, Baltimore, MD, Nov. 2004.
[21] *Haze Grey and Underway*. [Online]. Available: http://www.hazegray.org
[22] S. Zaidi, M. Hafeez, D. McLernon, and M. Ghogho, "A probabilistic model of *k*-coverage in minimum-cost wireless sensor networks," in *Proc. ACM CoNEXT Student Workshop*, Madrid, Spain, 2008, p. 33.
[23] *StarOddi*, Nov. 1, 2009. [Online]. Available: http://www.star-oddi.com
[24] *Woods Hole Oceanographic Institution*. [Online]. Available: http://www.whoi.edu/
[25] *Military Heat*, Nov. 1, 2009. [Online]. Available: http://www.military-heat.com

Gokhan Isbitiren received the B.S. and M.S. degrees in electrical and electronics engineering from the Middle East Technical University, Ankara, Turkey, in 2006 and 2009, respectively.

His research interests include underwater sensor networks, smart grid, and feeder automation.

Ozgur B. Akan (M'00–SM'07) received the B.S. degree in electrical and electronics engineering from Bilkent University, Ankara, Turkey, in 1999, the M.S. degree in electrical and electronics engineering from the Middle East Technical University, Ankara, in 2001, and the Ph.D. degree in electrical and computer engineering from the Georgia Institute of Technology, Atlanta, in 2004.

He is currently an Associate Professor with the Department of Electrical and Electronics Engineering, Koc University, Istanbul, Turkey, where he is also the Director of the Next-Generation and Wireless Communications Laboratory. He is the Associate Editor for the *International Journal of Communication Systems* (Wiley), the *European Transactions on Telecommunications*, and the *Nano Communication Networks Journal* (Elsevier). He was an Area Editor for the *Ad Hoc Networks Journal* (Elsevier) from 2004 to 2008, an Editor for the *ACM/Springer Wireless Networks Journal* from 2004 to 2010, and a Guest Editor for several special issues. His research interests include wireless communications, acoustic communications, nanocommunications, and information theory.

Dr. Akan is a Senior Member of the IEEE Communications Society, a Member of the Association for Computing Machinery (ACM), and the Vice President for IEEE Communications Society–Turkey Section. He is a Distinguished Lecturer of the IEEE Communications Society (COMSOC) for 2011 to 2012. He is the Associate Editor for the IEEE TRANSACTIONS ON VEHICULAR TECHNOLOGY. He is a Technical Program Committee (TPC) Cochair of the 16th IEEE Symposium on Computers and Communications and the 13th ACM International Conference on Modeling Analysis and Simulation of Wireless and Mobile Systems. He is a General Cochair for the Third International Conference on Bio-Inspired Models of Network, Information, and Computing Systems, the European Vice-Chair for the Second International Conference on Nano-Networks, and an International Vice-Chair for the 25th IEEE International Conference on Computer Communications. He has also served in organizing committees and TPCs of several other international conferences. He received the 2008 Turkish Academy of Sciences Distinguished Young Scientist Award, the 2008 and 2010 IBM Faculty Awards, and the 2010 IEEE COMSOC Outstanding Young Researcher Award (as a runner-up).